J. Biochem. 2012;151(4):439–446 doi:10.1093/jb/mvs012

JB THE JOURNAL OF BIOCHEMISTRY

PUGNAc treatment leads to an unusual accumulation of free oligosaccharides in CHO cells

Received October 10, 2011; accepted December 25, 2011; published online February 15, 2012

Ali Mehdy, Willy Morelle, Claire Rosnoblet, Dominique Legrand, Tony Lefebvre, Sandrine Duvet and François Foulquier*

IFR147, UMR8576 CNRS Laboratoire de Glycobiologie Structurale et Fonctionnelle, USTL, Villeneuve D'Ascq, France

*François Foulquier, UMR8576 CNRS, Glycobiologie Structurale et fonctionnelle, IFR 114, Bâtiment C9, USTL, 59655 Villeneuve D'Ascq Cedex, France. Tel: +33-320434430, Fax: +33-320436555, email: francois.foulquier@univ-lille1.fr

Free oligosaccharides (fOS) are generated as the result of *N*-glycoproteins catabolism that occurs in two distinct principal pathways: the endoplasmic reticulum-associated degradation (ERAD) of misfolded newly synthesized *N*-glycoproteins and the mature *N*-glycoproteins turnover pathway. The *O*-(2-acetamid*O*-2-deoxy-D-glucopyranosylidene) amino-*N*-phenylcarbamate (PUGNAc) is a potent inhibitor of the *O*-GlcNAcase (OGA) catalysing the cleavage of β-*O*-linked 2-acetamido-2-deoxy-β-D-glucopyranoside (*O*-GlcNAc) from serine and threonine residues of post-translationaly *O*-GlcNAc modified proteins. In order to estimate the impact of *O*-GlcNAc modification on *N*-glycoproteins catabolism, fOS were analysed by mass spectrometry (MS). MS analysis revealed the appearance of an unusual population of fOS after PUGNAc treatment. The structures representing this population have been identified as containing non-reducing end GlcNAc residues resulting from incomplete lysosomal fOS degradation. Only observed after PUGNAc treatment, the NButGt, another OGA inhibitor, did not lead to the appearance of this population. These abnormal fOS structures have clearly been shown to accumulate in membrane fractions as the consequence of lysosomal β-hexosaminidases inhibition by PUGNAc. As lysosomal storage disorders (LSD) are characterized by the accumulation of storage material as fOS in lysosomes, our study evokes that the use of PUGNAc could mimic a LSD. This study clearly points out another off target effects of PUGNAc that need to be taken into account in the use of this drug.

Keywords: degradation/lysosomes/mass spectrometry/oligosaccharide.

Abbreviations: CHO, Chinese Hamster Ovaries; ERAD, endoplasmic reticulum-associated degradation; fOS, free oligosaccharides; PUGNAc, *O*-(2-acetamido-2-deoxy-D-glucopyranosylidene) amino-*N*-phenylcarbamate.

N-Glycosylation can be considered as one of the most important post-translational modification of secreted and membrane proteins. Starting in the ER lumen by the transfer of an oligosaccharide $Glc_3Man_9GlcNAc_2$ from the mature lipid linked oligosaccharide precursor $Glc_3Man_9GlcNAc_2$-PP-Dolichol onto proteins, the *N*-linked oligosaccharides will then undergo extensive processing in the ER lumen by a range of glycosidases, such as glucosidases and mannosidases (*1*). The different generated glycan structures will serve as recognition tags for protein folding, endoplasmic reticulum-associated degradation (ERAD) and exit of glycoproteins from the ER (*1*).

Associated to the *N*-glycosylation process, soluble-free oligosaccharides (fOS) can be found in several types of animal cells. Their origin is still a debate but two main pathways have clearly been identified. First, fOS can arise from the ER degradation pathway of newly synthesized glycoproteins named ERAD. This pathway leads to the release of cytosolic fOS by the cytosolic peptide:*N*-glycanase (PNGase) (*2*). The resulting fOS bearing the di-*N*-acetylchitobiose (fOSGN2) are then subsequently hydrolysed by a cytosolic endo-β-*N*-acetylglucosaminidase (ENGase) to produce fOS with a single GlcNAc residue (fOSGN1) (*3*). The Man9-8GlcNAc1 structures are further trimmed by the cytosolic mannosidase Man2C1 (*4*) to generate a specific linear isomer of Man5GlcNAc1 [Manα1-2Manα1-2 Manα1-3(Manα 1-6)Manβ1-4GlcNAc] before being transported to the lysosomes by an ATP-dependent, high-affinity oligosaccharide transporter (*5*).

Although the above outlined scheme is well accepted, fOS can also arise as digestion intermediates during the lysosomal degradation of mature *N*-glycoproteins. This catabolism is part of the normal turnover of mature *N*-glycoproteins and contributes to the cellular homeostasis of glycosylation by recycling amino acids as well as monosaccharides. The pathway for their breakdown involves the concerted action of about 20 hydrolytic enzymes and occurs bidirectionally with the sequential release of monosaccharides by exoglycosidases from the non-reducing end of the oligosaccharide chains. Concomitantly, a set of hydrolytic events then digests the polypeptide chain and the protein–carbohydrate linkage region by a glycosyl asparaginase that first requires the removal of fucose residue by α-L-fucosidase (*6*). The release of the *N*-acetylglucosamine residue of the chitobiose and the hydrolysis of Manβ1-4GlcNAc linkage at the reducing end is, respectively, achieved by an endo-β-*N*-acetylglucosaminidase or lysosomal di-*N*-chitobiobiase present both in humans and rodents, and β-mannosidase (*6*). The breakdown of the

oligosaccharide from the non-reducing end requires the action of *N*-acetyl-β-D-hexosaminidases (lysosomal β-hexosaminidases) that catalyses the removal of *N*-acetylglucosamine residues. Other specific exoglycosidases will also be required such as α-neuraminidase, β-galactosidase and α-mannosidase (*6*).

Besides the *N*-glycosylation process, a large number of cytoplasmic and nuclear proteins have been reported to be post-translationally modified by *N*-acetylglucosamine (*O*-GlcNAc) on specific serine/threonine residues. This highly dynamic modification is catalysed by an *O*-GlcNAc transferase enzyme (OGT), and removed by the antagonistic enzyme β-*N*-acetylglucosaminidase (*O*-GlcNAcase, OGA) (*7*). For the past decade, *O*-(2-acetamido-2-deoxy-D-glucopyranosylidene) am ino-*N*-phenylcarbamate (PUGNAc), human *O*-GlcNA case inhibitor, has been widely used to increase cellular *O*-GlcNAc levels and to evaluate the cellular function(s) played by the post-translational modification *O*-Glc NAc (*8*). It later became apparent that PUGNAc shows weak selectivity for OGA while the *N*-butyl thiazoline (NbutGT) and very likely other inhibitors have greater selectivity for OGA (*9*).

In our current study, we looked for evidences implicating *O*-GlcNAc modification in the *N*-glycoproteins' degradation pathways. In order to tackle this relationship, we have explored the quality and quantity of fOS in PUGNAc CHO-treated cells. Mass spectrometry (MS) analysis revealed the appearance of an unusual population of fOS after PUGNAc treatment. The structures represented in this population have been identified as containing non-reducing end GlcNAc residues resulting from incomplete lysosomal fOS degradation in *CHO* cells. These structures clearly accumulate in membrane fractions as the consequence of lysosomal β-hexosaminidases inhibition.

Materials and Methods

Cell culture

Pro-5 CHO cell line was cultured in α-minimal essential medium (Gibco) supplemented with 10% (v/v) fetal bovine serum and 2.5 mM L-glutamine at 37°C under 5% CO_2 and plated in 175 cm^2 dishes. CHO cells, grown until confluence, were incubated or not, before analysis, with 100 μM of PUGNAc (Sigma Aldrich, St Quentin Fallavier) or with NbutGT inhibitor (100 μM) that was kindly provided by Dr David J. Vocadlo.

Immunoblotting

An amount of 20 μg of proteins were analysed by SDS–PAGE and immunoblotted with Anti-*O*-GlcNAc (RL2) (1:10000) and anti-α-tubulin obtained both from Sigma-Aldrich Co. (St Louis, MO, USA). Cells were washed twice on ice (Santa Cruz Biotechnology) with cold PBS (phosphate-buffered saline) and then lysed for 5 min on ice in cell lysis buffer (25 mM Tris–HCL, 150 mM NaCl, pH 7.6, supplemented with 1% Triton X-100, 1% sodium deoxycholate and 0.1% SDS). Proteins were quantified by using the Micro BSA Protein Assay Kit (Thermo Fisher Scientific, Brebieres, France). Signals were detected using the ECL plus detection Kit (Amersham Biosciences, UK) according to the manufacturer's instructions.

Preparation of cytosolic and membrane fractions

CHO cells treated or not with PUGNAc, were cultured in 175 cm^2 dishes. Once confluent ($\sim 20 \times 10^6$ cells), cells were washed twice on ice (Santa Cruz Biotechnology) with cold PBS (phosphate-buffered saline) and then scraped in 300 μl of KMH buffer (110 mM potassium acetate, 2 mM magnesium acetate, 20 mM HEPES, pH 7.2) containing protease inhibitor cocktail (cOmplete; Roche Diagnostics). After homogenization by using a ball-bearing-type homogenizer, cells were centrifuged for 1 h at $105{,}000 \times g$. The resulting supernatant is referred as the cytosolic fraction and the pellet as the membrane fraction. Both fractions were then submitted to lipid extraction by addition of 3 ml of $CHCl_3$/MeOH/H_2O (3/2/1, v/v/v). The aqueous phases resulting from the lipid extraction were then lyophilized. The remaining glycoproteins pellet was dried in a vacuum centrifuge.

Release of the N-linked oligosaccharides and clean-up procedure of the PNGase F-released N-glycans

The dried protein pellet was dissolved in 200 μl of 50 mM ammonium bicarbonate containing 0.25% w/v SDS and 0.25% v/v β-mercaptoethanol and subsequently heated for 20 min at 100°C. After adding 200 μl of 50 mM ammonium bicarbonate in the cooled samples, 20 μl of 10% v/v Nonidet P40 and 3 U of PNGase F were successively added and the deglycosylation was incubated at 37°C for 18 h. The PNGase F digestion was terminated by drying *in vacuo*. The *N*-glycans were desalted on a column of 150 mg of non-porous graphitized carbon (Alltech, Deerfield, IL, USA). The column was sequentially washed with 5 ml methanol and 10 ml 0.1% v/v TFA. The *N*-glycans were dissolved in 1 ml of 0.1% v/v TFA, applied to the column and washed with 3×5 ml of 0.1% v/v TFA. The elution of *N*-glycans was conducted with the application of 5 ml of 25% v/v ACN in water containing 0.1% v/v TFA. The fraction was freeze-dried. β-Hexosaminidase digestion was carried out at 37°C for 48 h with 50 U/ml in 50 mM ammonium formate pH 4.6. The samples were lyophilized and then permethylated before MALDI–MS analysis.

Permethylation of the glycans

Permethylation of the freeze-dried PNGase F-released *N*-glycans and soluble oligosaccharides was performed according to the procedure developed by Ciucanu and Kerek (*10*) .The reaction was stopped by adding 1 ml of cold 5% v/v acetic acid followed by three extractions with 500 μl of chloroform. The pooled chloroform phases (1.5 ml) were then washed eight times with ultra-pure water. The methylated derivatives-containing chloroform phase was finally dried under a stream of nitrogen and the extracted products were further purified on a C18 Sep-Pak. The C18 Sep-Pack was sequentially conditioned with methanol (5 ml), and water (2×5 ml). The derivatized glycans dissolved in methanol were applied on the cartridge, washed with 3×5 ml water, 2 ml of 10% v/v ACN in water and eluted with 3 ml of 80% v/v ACN in water. ACN was evaporated under a stream of nitrogen and the samples were freeze-dried.

MALDI -MS analysis of permethylated glycans

MALDI–MS experiments were carried out on voyager Elite DE-STR Pro instrument (PersSeptive Biosystem, Fanmingham, MA, USA) equipped with a pulsed nitrogen laser (337 nm) and a gridless delayed extraction ion source. The spectrometer was operated in positive reflectron mode by delayed extraction with an accelerating voltage of 20 kV and a pulse time of 200 ns and grid voltage of 66%. All the spectra shown represent accumulated spectra obtained by 400–500 laser shots. Sample was prepared by mixing a 1 μl aliquot (5–10 pmol) with 1 μl of matrix solution, on the MALDI sample plate. The matrix solution was prepared by saturating a methanol–water (1:1) with DHB (10 mg/ml).

Relative quantification

Relative quantification analysis of permethylated fOS was performed as previously described (*11*). Oligosaccharides were first released and peremethylated from a fixed amount of cells (20×10^6). For the internal standard, 30 μg of dried Galβ1-4GlcNAc were suspended in dimethyl sulphoxide (DMSO) (0.1 ml) and NaOH (20 mg in 0.1 ml of dry DMSO) was added. After strong mixing, 0.1 ml of ^{13}C-labelled methyl iodide (Aldrich, St Louis, MO, USA) was added. The ^{13}C-labelled methylated oligosaccharide has been purified according to Alvarez-Manilla and collaborators (*11*) and dissolved in 50% methanol at the final concentration of 10 μg/ml.

The MALDI–MS matrix was then prepared by saturating a methanol–water (1:1) with DHB (10 mg/ml). Then, 0.5 ml of methylated glycan sample was mixed with 0.5 ml of matrix solution and 0.5 ml of ^{13}C-labelled methylated oligosaccharide. The spectrometer

was operated in positive reflectron mode by delayed extraction with an accelerating voltage of 20 kV and a pulse time of 200 ns and grid voltage of 66%. All the spectra shown represent accumulated spectra obtained by 400–500 laser shots. For each condition, three samples were spotted and the amount of each oligosaccharide was relatively quantified and estimated by calculating the ratio between the relative amount of these oligosaccharides and the internal standard in the MALDI–MS spectra.

Results

PUGNAc inhibitor causes an increase of O-GlcNAc modified proteins level and the appearance of an unusual fOS population in CHO cells

PUGNAc and NButGT are well-known potent OGA (*O*-GlcNAcase) inhibitors. In order to assess the inhibitory efficacy of these two inhibitors towards OGA, the *O*-GlcNAc modified proteins level was assessed by western blot (Fig. 1). In contrast to untreated CHO cells, cells treated either with PUGNAc or NbutGT showed a marked increase of *O*-GlcNAc modified proteins level stemming from the continuing action of OGT while *O*-GlcNAcase functions are hindered (Fig. 1).

In order to determine the impact of *O*-GlcNAc-modified proteins on the catabolic pathways of *N*-glycoproteins, fOS have been analysed by MS in CHO control cells and CHO cells treated with PUGNAc and NbutGT, respectively. MS profiling of permethylated fOS representing the total soluble oligosaccharides isolated from CHO control cells (A) and from CHO treated separately with PUGNAc (B) and NbutGT (C) was shown in Fig. 2. The structures shown in the annotations were assigned from

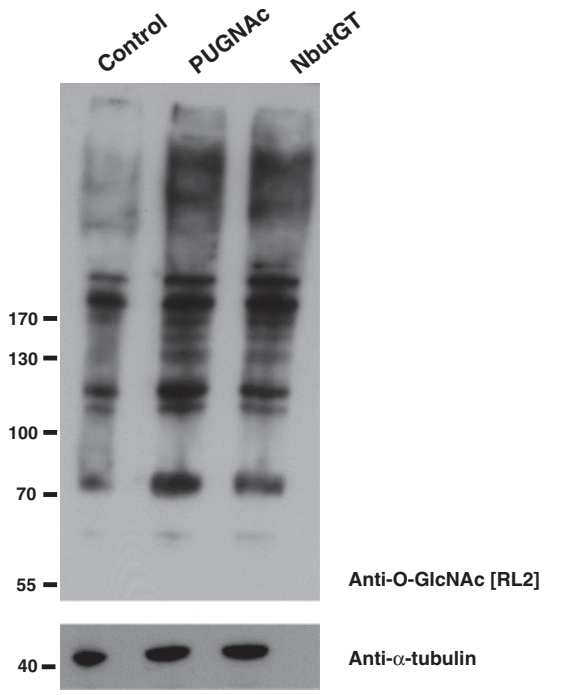

Fig. 1 O-GlcNAc protein levels in Pro-5 CHO cells treated or not with PUGNAc or NButGT. *Pro-5* CHO cells were treated over night with 100 μM of PUGNAc and 100 μM of NButGT, respectively. *O*-GlcNAc modified protein levels were analysed by western blot (upper panel). Western blot analysis of cellular α-tubulin levels shows equal loading for the three lanes (lower panel).

compositional information provided by the MAL DI–MS data. The representative MS profile of total fOS from CHO control cells in Fig. 2A shows a population of Hex1-5HexNAc1 type oligosaccharides with one single HexNAc residue at *m*/*z* 518 (Hex1HexNAc1), *m*/*z* 722(Hex2HexNAc1), *m*/*z* 926(Hex3HexNAc1), *m*/*z* 1130 (Hex4HexNAc1), *m*/*z* 1334(Hex5HexNAc1) and *m*/*z* 1538 (Hex6HexNAc1), the major ion was observed at *m*/*z* 518. Surprisingly, the MALDI–MS profile of total fOS from CHO–PUGNAc-treated cells (Fig. 2B) consisted in a heterogeneous population of fOS compared with the one obtained from CHO control cells. The most notable features of the data indicate the appearance of an unusual fOS population in CHO cells bearing 2–5 HexNAc residues observed at *m*/*z* 967 (Hex2HexNAc2), *m*/*z* 1170 (Hex3HexNAc2), *m*/*z* 1416 (Hex3HexNAc3), *m*/*z* 1662 (Hex3HexNAc4) and *m*/*z* 1907 (Hex3HexNAc5) in addition to the fOS population possessing only one single HexNAc residue to their reducing end and observed in CHO control cells. At the opposite, the MALDI–MS profile of the total fOS obtained from NbutGT CHO treated cells (Fig. 2C) did not reveal the presence of this fOS population bearing 2–5 HexNAc residues. Hence, these data indicate that the appearance of the unusual fOS population bearing 2–5 HexNAc residues observed after PUGNAc treatment is not due to a selective OGA inhibition.

fOS structures accumulating in PUGNAc-treated CHO cells are located in the membrane fraction and bear only one GlcNAc residue at their reducing end

In order to evaluate the subcellular distribution of fOS in PUGNAc CHO-treated cells, cytosolic fOS and fOS located in the membrane fractions were separated by ultracentrifugation (Fig. 3). MALDI–MS analysis of permethylated cytosolic and membrane fOS fraction derived from control and PUGNAc-treated CHO cells were performed. The MALDI–MS profiles of permethylated cytosolic oligosaccharides from CHO control and from PUGNAc CHO-treated cells were depicted, respectively, in Fig. 3A and C. The cytosolic fOS of CHO cells treated with PUGNAc or not treated remain unchanged and appear to have the same MALDI–MS profiles. As was the case for the total fOS derived from control cells in Fig. 1A, the MALDI–MS profiles of cytosolic fOS fraction with or without PUGNAc treatment show the same molecular ions corresponding to the population of Hex1-5HexNAc1. The MALDI–MS profiles of membrane fOS fraction derived from control and from PUGNAc CHO-treated cells were shown, respectively, in Fig. 3B and D. The MALDI–MS profiles of cytosolic and membrane fOS fractions in CHO cells show the same profiles. In contrast, comparison of MS profiles of cytosolic and membrane fOS after PUGNAc treatment revealed the presence of Hex2HexNAc2, Hex3HexNAc2, Hex3HexNAc3, Hex3HexNAc4 and Hex3HexNAc5 species in membrane fraction. These findings clearly demonstrate that PUGNAc has no effect on the cytosolic fOS structures but strongly affects the fOS structures located in the membrane fraction. To determine whether these oligosaccharides are containing one or two intact GlcNAc residues at their

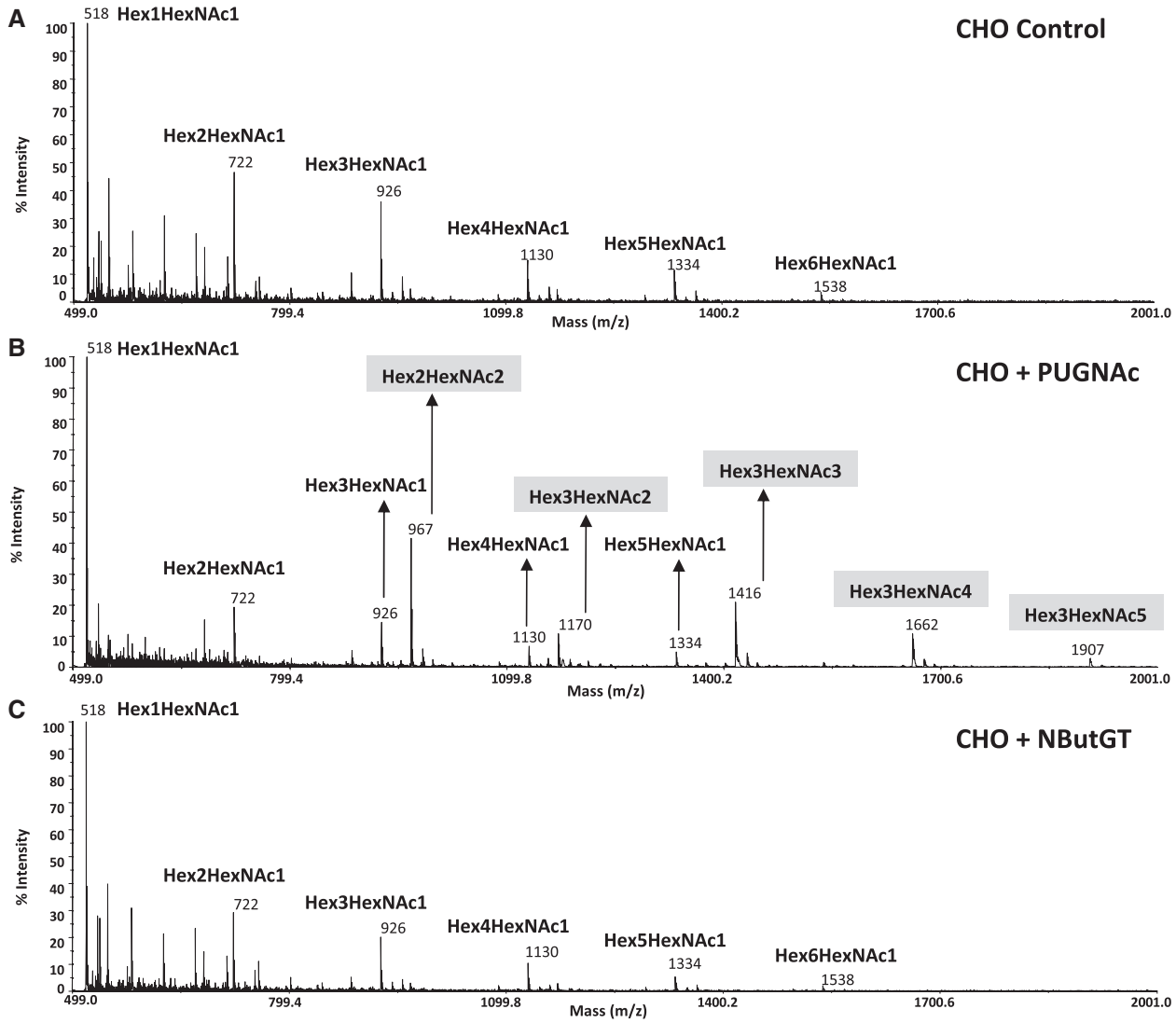

Fig. 2 fOS structures accumulate in PUGNAc-treated CHO cells. MALDI–MS profiles of permethylated total oligosaccharides from CHO controls cells (A), CHO treated separately with 100 μM of PUGNAc (B) and with 100 μM of NbutGT (C). fOS are derived from the 50% (v/v) acetonitrile fraction from a C18 Sep-Pak. All molecular ions are [M + Na]+, and nominal masses of 12C isotope are shown.

reducing end, fOS population followed PUGNAc treatment was characterized structurally using β-hexosaminidase activity. After β-hexosaminidase treatment (Fig. 4B), the $[M + Na]^+$ ions at *m/z* 967 (Hex2HexNAc2), *m/z* 1170 (Hex3HexNAc2), *m/z* 1416 (Hex3HexNAc3), *m/z* 1661 (Hex3HexNAc4) and *m/z* 1906 (Hex3HexNAc5) disappeared, concomitantly, with the appearance of a major ion at *m/z* 926 (Hex3HexNAc1). These data indicate that, as expected, non-reducing GlcNAc residues were fully trimmed to form the Hex3HexNAc1 structure possessing an intact single GlcNAc residue at the reducing end.

PUGNAc has no effect on N-linked glycan structures

In order to check whether the structure of the glycan moiety on glycoproteins was changed by PUGNAc treatment, the detailed structural analysis of *N*-glycans released from total *N*-glycoproteins in PUGNAc CHO-treated cells was performed. MALDI–MS analysis of permethylated PNGase F released *N*-glycans from total cellular extracts of CHO control cells (Fig. 5A) and PUGNAc CHO-treated cells (Fig. 5B) has been performed. In both MALDI–MS spectra, assigned compositions of *N*-glycans are consistent with complex-type glycans (dHex0-1Hex5-9HexNAc2–7). The same molecular ions were observed in the spectra of global permethylated PNGase F released *N*-Glycans from both untreated and PUGNAc treated CHO demonstrating that PUGNAc has no effect on *N*-linked glycan structures.

Relative quantification of fOS

In order to establish a relative quantitative profiling of fOS in both control and PUGNAc-treated cells, fOS were analysed for their relative abundances (Fig. 6). To achieve this relative quantification, the permethylated fOS were mixed with a known amount of ^{13}C-labelled methylated oligosaccharide as an internal standard, and freeze-dried before MALDI–MS analysis. The amount of each oligosaccharide was relatively

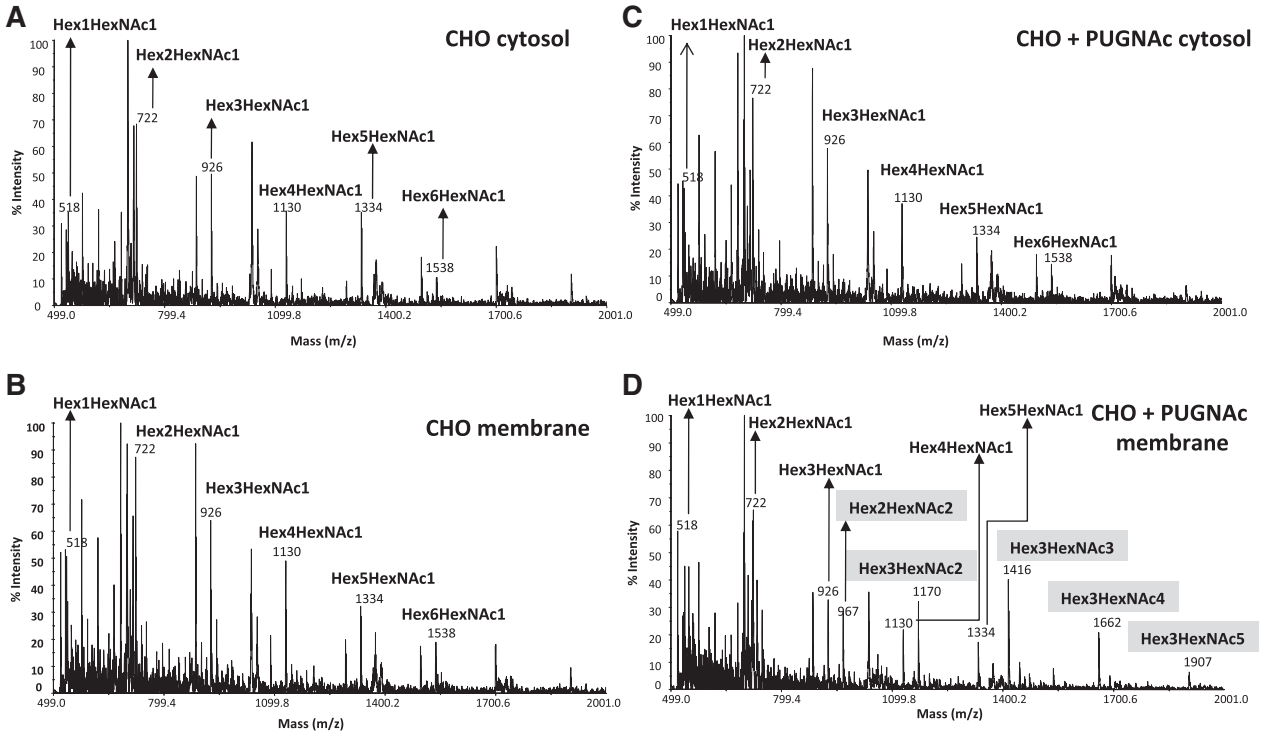

Fig. 3 Subcellular localisation of the fOS population observed after PUGNAc treatment. Cytosolic fractions from CHO control (A) and from CHO–PUGNAc-treated cells (B), membrane fractions from CHO control (C) and from CHO–PUGNAc-treated cells of fOS were obtained by ultracentrifugation. The permethylated fOS of each fraction were analysed by MALDI.

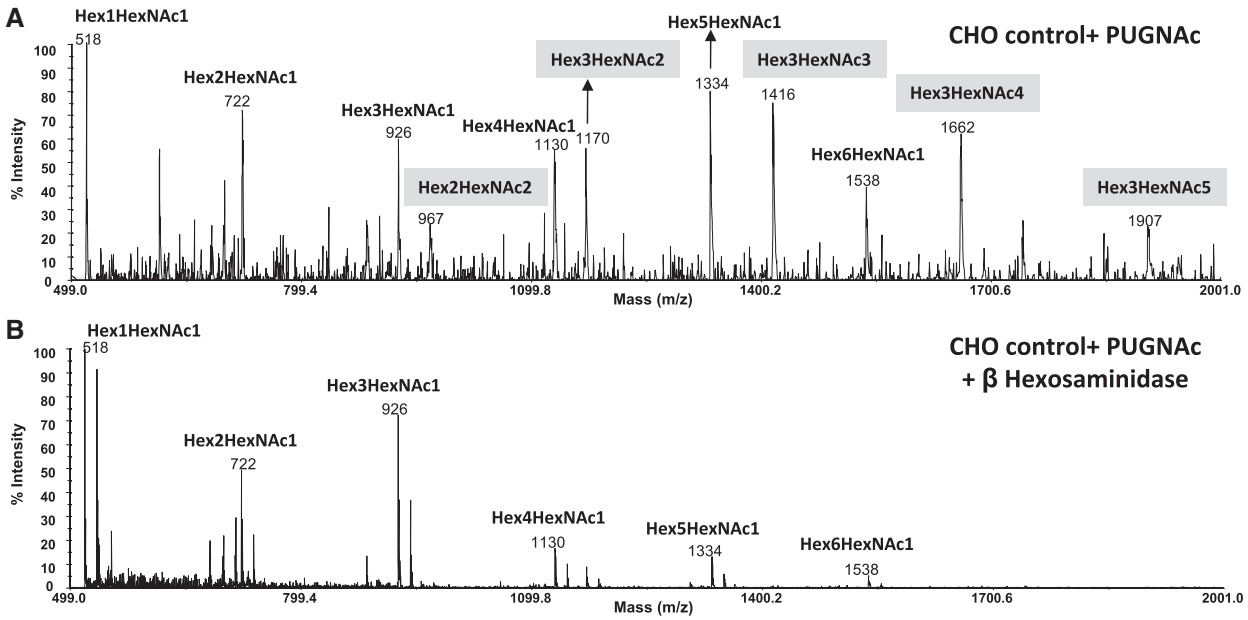

Fig. 4 Beta-hexosaminidase treatment on fOS population followed PUGNAc treatment. MALDI–MS profiles of permethylated fOS from CHO–PUGNAc treated cells (A), and after treatment with β-*N*-acetylhexosaminidase (B). After purification on a non-porous graphitized carbon SPE cartridge, the fOS were analysed in positive ion reflective mode after on-target exoglycosidase digestion, as $[M + Na]^+$ pseudomolecular ions.

quantified and estimated by calculating the ratio between the relative amount of these oligosaccharides and the internal standard observed at m/z 542 in the MALDI–MS spectra of both control and PUGNAc CHO treated cells. As observed in Fig. 6, in CHO cells treated or not with PUGNAc, the Hex1HexNAc1 structure is the most abundant, although 4-fold increased after PUGNAc treatment. Interestingly, the population of oligosaccharides with 2–5 GlcNAc residues only appears in CHO–PUGNAc-treated cells in which the major oligosaccharide is the Hex3HexNAc3. Compared with untreated CHO cells, this population clearly accumulates after PUGNAc treatment.

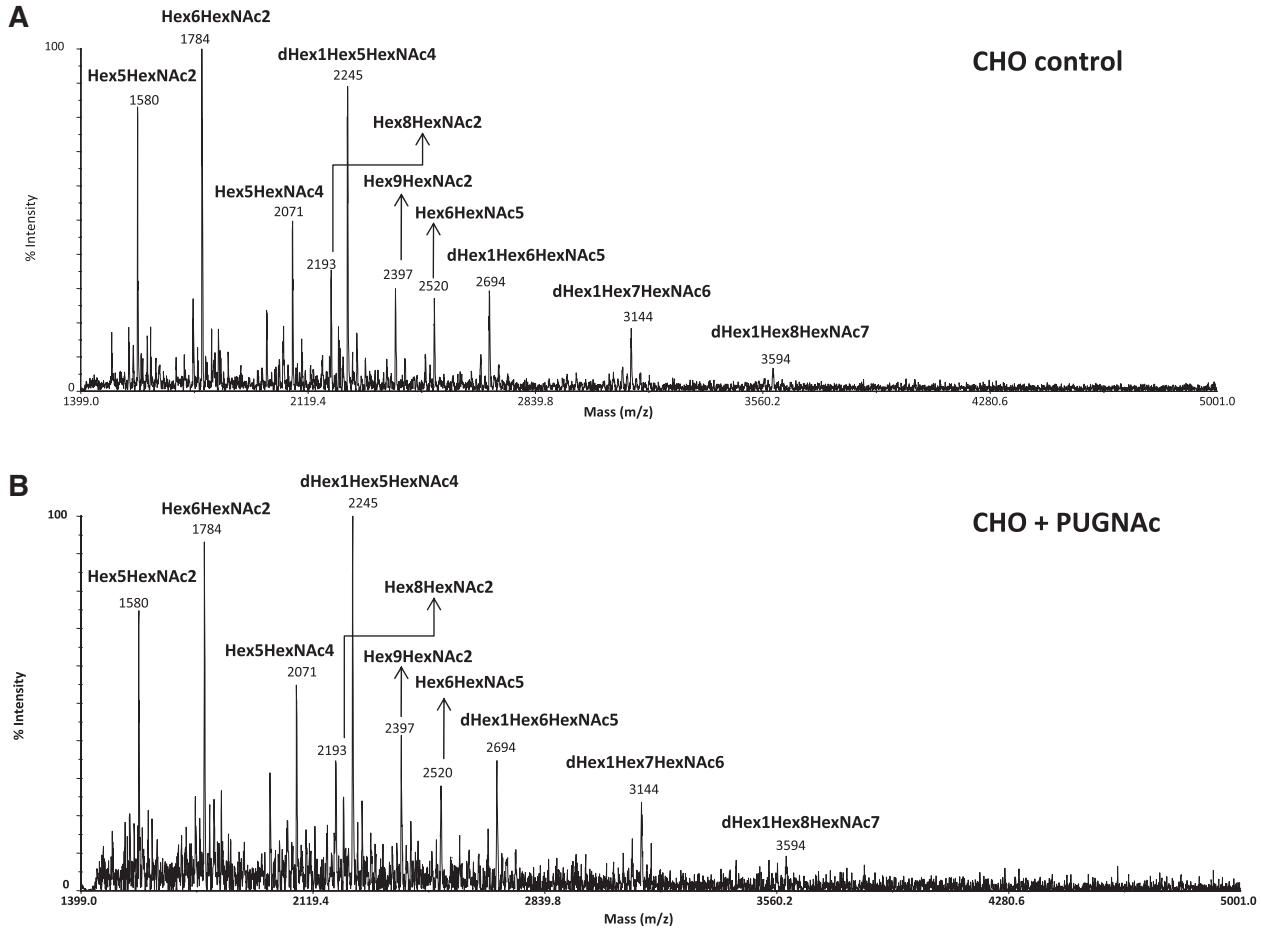

Fig. 5 N-linked glycan structures followed PUGNAc treatment. MALDI–MS profiles of PNGase F-released *N*-glycans from CHO control (A) and CHO–PUGNAc-treated cells (B). Glycans were released from the resulting peptides/glycoproteins by digestion with PNGase F. PNGase F-released *N*-glycans were separated from peptides using a C18 Sep-Pak. The glycans were permethylated and then analysed in positive reflective mode as [M + Na +] pseudomolecular ions.

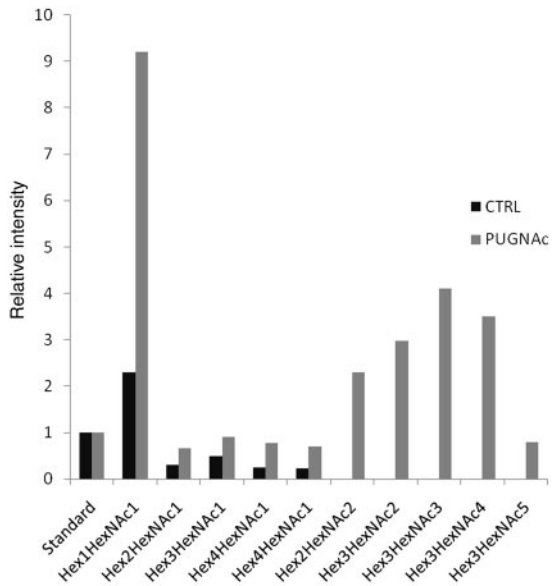

Fig. 6 Relative quantities of permethylated fOS in untreated and PUGNAc-treated CHO cells. The amount of each oligosaccharide was relatively quantified and estimated by calculating the ratio between the relative amount of these oligosaccharides and a known quantity of ^{13}C-labelled methylated oligosaccharide as internal standard in the MALDI–MS profiles.

Discussion

N- and *O*-linked β-*N*-acetylglucosaminylation glycosylations are two major post-translational modifications occurring for the first one on membrane and secreted proteins and for the second one, on cytosolic and nuclear proteins. In our current study, we looked for evidences implicating *O*-GlcNAc modification in the metabolism of *N*-glycoproteins and more particularly on its catabolism. Insights into fOS metabolism is a powerful way to rapidly obtain a complete and comprehensive source of information highlighting the *N*-glycoproteins degradation pathway. The presence of fOS has been reported in several types of animal cells either in the cytosol or in lysosomes (*12–20*). Changes and/or differences in their structures are generally the result of differences in their biosynthetic pathways. In several lysosomal storage disorders (LSDs), the accumulated fOS have been structurally characterized and allowed to delineate the defective enzyme(s) or pathways.

MALDI–MS technique was used to characterize the total fOS structures extracted from untreated and PUGNAc CHO-treated cells. When CHO cells were exposed to PUGNAc, a significant amount of an unusual fOS population was observed in addition to

the population of Hex(*1*–*7*)HexNAc1 already observed in absence of PUGNAc. To elucidate the structures of these fOS, specific and targeted exoglycosidase digestion was carried out and the products were monitored with MALDI–MS. Such analysis demonstrated the presence of structures containing non-reducing GlcNAc residues with a single GlcNAc residue at the reducing end. These structures are in accordance with an incomplete degradation of fOS in lysosomes due to β-lysosomal hexosaminidases inhibition. In contrast to PUGNAc, we observed that NbutGT did not lead to such population demonstrating that this population was not due to a selective OGA inhibition. As expected, these species were not found in the cytosol, but in the membrane fraction where they accumulate. In addition, mass spectrometric *N*-glycan profiling revealed no significant changes of the total *N*-glycan pattern after PUGNAc treatment demonstrating that the biosynthetic pathway of *N*-glycoproteins was not affected by PUGNAc.

PUGNAc has been used in over 50 studies in order to investigate the effect of increased *O*-GlcNAc levels in variety of cell lines, and most particularly to induce insulin resistance (*21*–*23*). The 3T3-L1 adipocytes cells which are considered as a standard model cell line for diabetes research, showed an insulin resistance after PUGNAc treatment associated with an impaired akt phosphorylation (*23*). Surprisingly, Vocadlo and collaborators (*24*) showed that the selective *O*-GlcNAcase inhibitor NbutGT was unable to reproduce the insulin resistance effects of PUGNAc on cultured 3T3-L1 adipocyte. Regarding these observations, it has been suggested that elevated *O*-GlcNAc levels are not correlated with PUGNAc phenotype in these experiments, so that the lack of selectivity or other potential off-target effects of PUGNAc should be considered in studies making use of PUGNAc to reproduce increases in *O*-GlcNAc levels.

PUGNAc is an inhibitor of both lysosomal β-hexosaminidase α- and β-subunits that are members of family 20 of glycosyl hydrolases and OGA. HEXA and HEXB are localized in lysosomes and hydrolyse terminal *N*-acetylglucosamine and *N*-acetylgalactosamine residues of glycosphingolipids and *N*-linked oligosaccharides. Vocadlo and collaborators have reported that the use of PUGNAc increased accumulation of the glycolipids GM2 (*25*). Our works demonstrate that PUGNAc also affects the structure of fOS resulting from the mature *N*-glycoproteins turnover pathway. As certain LSD are also characterized by the accumulation of storage material as fOS in lysosomes, our study evokes that PUGNAc could mimic a LSD and shows another off target effects that need to be taken into account in the use of this drug. While annoying for people working in the field of *O*-GlcNAc, this side effect could be used to investigate the quantitative importance of the catabolic turn over pathway versus ERAD pathway of *N*-glycoproteins.

Funding
Centre National de la Recherche scientifique (Unité Mixte de Recherche CNRS/USTL 8576; Director: Dr Jean-Claude Michalski); the Agence Nationale de la Recherche (ANR-JC-SWEET-CDG) (to F.F.); The Mass Spectrometry facility, European Community (FEDER); the Région Nord pas de Calais (France); Université des Sciences et Technologies de Lille 1.

Conflict of interest
None declared.

References

1. Helenius, A. and Aebi, M. (2004) Roles of N-linked glycans in the endoplasmic reticulum. *Annu. Rev. Biochem.* **73**, 1019–1049
2. Suzuki, T., Park, H., and Lennarz, W.J. (2002) Cytoplasmic peptide:N-glycanase (PNGase) in eukaryotic cells: occurrence, primary structure, and potential functions. *FASEB J.* **16**, 635–641
3. Pierce, R.J., Spik, G., and Montreuil, J. (1979) Cytosolic location of an endo-N-acetyl-beta-D-glucosaminidase activity in rat liver and kidney. *Biochem. J.* **180**, 673–676
4. Suzuki, T., Hara, I., Nakano, M., Shigeta, M., Nakagawa, T., Kondo, A., Funakoshi, Y., and Taniguchi, N. (2006) Man2C1, an alpha-mannosidase, is involved in the trimming of free oligosaccharides in the cytosol. *Biochem. J.* **400**, 33–41
5. Saint-Pol, A., Codogno, P., and Moore, S.E.H. (1999) Cytosol-to-lysosome transport of free polymannose-type oligosaccharides. Kinetic and specificity studies using rat liver lysosomes. *J. Biol. Chem.* **274**, 13547–13555
6. Winchester, B. (2005) Lysosomal metabolism of glycoproteins. *Glycobiology* **15**, 1–15
7. Hart, G.W., Haltiwanger, R.S., Holt, G.D., and Kelly, W.G. (1989) Glycosylation in the nucleus and cytoplasm. *Annu. Rev. Biochem.* **58**, 841–874
8. Hart, G.W., Slawson, C., Ramirez-Correa, G., and Lagerlof, O. (2011) Cross talk between O-GlcNAcylation and phosphorylation: roles in signaling, transcription, and chronic disease. *Annu Rev Biochem.* **80**, 825–858
9. Whitworth, G.E., Macauley, M.S., Stubbs, K.A., Dennis, R.J., Taylor, E.J., Davies, G.J., Greig, I.R., and Vocadlo, D.J. (2007) Analysis of PUGNAc and NAG-thiazoline as transition state analogues for human O-GlcNAcase: mechanistic and structural insights into inhibitor selectivity and transition state poise. *J. Am. Chem. Soc.* **129**, 635–44
10. Ciucanu, I. and Kerek, F. (1984) A simple and rapid method for the permethylation of carbohydrates. *Carbohydr. Res.* **131**, 209–217
11. Alvarez-Manilla, G., Warren, N.L., Abney, T., Atwood, J., Azadi, P., York, W.S., Pierce, M., and Orlando, R. (2007) Tools for glycomics: relative quantitation of glycans by isotopic permethylation using 13CH3I. *Glycobiology* **17**, 677–687
12. Anumula, K.R. and Spiro, R.G. (1983) Release of glucose-containing polymannose oligosaccharides during glycoprotein biosynthesis. Studies with thyroid microsomal enzymes and slices. *J. Biol. Chem.* **258**, 15274–15282
13. Cacan, R., Hoflack, B., and Verbert, A. (1980) Fate of oligosaccharide-lipid intermediates synthesized by resting rat-spleen lymphocytes. *Eur. J. Biochem.* **106**, 473–479
14. Cacan, R. and Verbert, A. (1999) Free and N-linked oligomannosides as markers of the quality control of newly synthesized glycoproteins. *Biochem. Biophys. Res. Commun.* **258**, 1–5

15. Cacan, R. and Verbert, A. (2000) Transport of free and N-linked oligomannoside species across the rough endoplasmic reticulum membranes. *Glycobiology* **10**, 645–648
16. Iwai, K., Mega, T., and Hase, S. (1999) Detection of Man5GlcNAc and related free oligomannosides in the cytosol fraction of hen oviduct. *J. Biochem.* **125**, 70–74
17. Kmiecik, D., Herman, V., Stroop, C.J.M., Michalsky, J.-C., Mir, A.-M., Labiau, O., Verbert, A., and Cacan, R. (1995) Catabolism of glycan moieties of lipid intermediates leads to a single Man5GlcNAc oligosaccharide isomer: a study with permeabilized CHO cells. *Glycobiology* **5**, 483–494
18. Moore, S.E.H. and Spiro, R.G. (1994) Intracellular compartmentalization and degradation of free polymannose oligosaccharides released during glycoprotein biosynthesis. *J. Biol. Chem.* **269**, 12715–12721
19. Ohashi, S., Iwai, K., Mega, T., and Hase, S. (1999) Quantitation and isomeric structure analysis of free oligosaccharides present in the cytosol fraction of mouse liver: detection of a free disialobiantennary oligosaccharide and glucosylated oligomannosides. *J. Biochem.* **126**, 852–858
20. Spiro, R.G. (2004) Role of N-linked polymannose oligosaccharides in targeting glycoproteins for endoplasmic reticulum-associated degradation. *Cell. Mol. Life Sci.* **61**, 1025–1041
21. Arias, E.B., Kim, J., and Cartee, G.D. (2004) Prolonged incubation in PUGNAc results in increased protein O-Linked glycosylation and insulin resistance in rat skeletal muscle. *Diabetes* **53**, 921–930
22. Yang, X., Ongusaha, P.P., Miles, P.D., Havstad, J.C., Zhang, F., So, W.V., Kudlow, J.E., Michell, R.H., Olefsky, J.M., Field, S.J., and Evans, R.M. (2008) Phosphoinositide signalling links OGlcNAc transferase to insulin resistance. *Nature* **451**, 964–969
23. Vosseller, K., Wells, L., Lane, M.D., and Hart, G.W. (2002) Elevated nucleocytoplasmic glycosylation by O-GlcNAc results in insulin resistance associated with defects in Akt activation in 3T3-L1 adipocytes. *Proc. Natl. Acad. Sci. USA* **99**, 5313–5318
24. Macauley, M.S., Bubb, A.K., Martinez-Fleites, C., Davies, G.J., and Vocadlo, D.J. (2008) Elevation of global O-GlcNAc levels in 3T3-L1 adipocytes by selective inhibition of O-GlcNAcase does not induce insulin resistance. *J. Biol. Chem.* **283**, 34687–34695
25. Stubbs, K.A., Macauley, M.S., and Vocadlo, D.J. (2009) A selective inhibitor Gal-PUGNAc of human lysosomal beta-hexosaminidases modulates levels of the ganglioside GM2 in neuroblastoma cells. *Angew Chem. Int. Ed.* **48**, 1300–1303